DOI: 10.1002/cphc.201200968

Tomographic Reconstruction of Designer Free-Electron Wave Packets

Matthias Wollenhaupt,*[a] Christian Lux,[a] Marc Krug,[b] and Thomas Baumert[a]

We review the generation and tomographic reconstruction of designer electron wave packets, that is, electron wave packets with a tailored momentum distribution in the continuum. Generation is accomplished by means of multiphoton ionization of an atomic prototype using polarization-shaped femtosecond laser pulses. Both the electronic structure of the neutral and interference of matter wave packets in the continuum contribute to the final shape. For the measurement of the resulting three-dimensional photoelectron angular distributions (3dPAD) we combine the established technique of velocity map imaging (VMI) with a tomographic reconstruction method. This novel experimental approach can be employed to characterize the 3dPAD in the laboratory frame as well as in the molecular frame of larger molecules. Due to its sensitivity to electronic structure this method can be further developed to highly sensitive analytic techniques in the gas phase, for instance for the identification of chiral molecules.

1. Introduction

Albert Einstein's theory of the photoelectric effect has contributed significantly to the development of quantum physics. In his famous "Annus Mirabilis" paper *On a Heuristic Point of View about the Creation and Conversion of Light* Einstein wrote in 1905: "energy quanta penetrate into a surface layer of the body, and their energy is at least partly transformed into electron kinetic energy. The simplest picture is that a light quantum transfers all of its energy to a single electron […]. An electron obtaining kinetic energy inside the body will have lost part of its kinetic energy when it has reached the surface. Moreover, we must assume that each electron on leaving the body must produce work W, which is characteristic for the body. Electrons which are excited at the surface and at right angles to it will leave the body with the greatest normal velocity. The kinetic energy of such electrons is $h\nu - W$"[1].[1] In the same work he also referred to the experiments on the photoelectric effect by Philipp Lenard. Lenard used arc and spark lamps for illumination, electrometric methods and fluorescence screens in simple vacuum tubes for detection to discover the fundamental physical law of the photoelectric effect, namely that the number of electrons increases with increasing light intensity, but energy of the electrons does not.

The central role of the photoelectric effect in basic research was underscored by the 1981 Nobel Prize in physics awarded to Kai Siegbahn for "his contribution to the development of high-resolution electron spectroscopy". Nowadays, arc and spark lamps have been replaced by modern light sources such as lasers, synchrotrons and free-electron lasers. Also, modern detection techniques comprise advanced time- and position-sensitive detectors instead of fluorescence screens. For example, in surface science, the electronic structure of new materials is routinely investigated by photoelectron spectroscopy; in molecular physics, femtosecond techniques are employed to observe[3,4] and control[5] intramolecular dynamics of isolated molecules; in atomic physics inner-shell excitation and the subsequent dynamics has been measured down to the attosecond time scale.[6] In addition, the electric fields achievable by intense laser pulses exceed those of the electronic bonds in molecules, giving rise to field-driven ionization. While it was sufficient for the interpretation of the initial experiments on the photoelectric effect to consider the electrons as particles, the wave nature of the electrons was demonstrated by Clinton Davisson and Lester Germer in 1927[7] in their famous scattering experiments on nickel.

Nowadays, pulsed light sources are often used for photoionization and thus the notion of the photoelectron as a free wave packet comes to the fore. As wave packets consist of the superposition of many waves, the exciting question arises whether those matter wave packets can be "designed" in the exact same manner as in Fourier synthesis. This question can be addressed by modern methods of ultrashort laser physics. Due to the uncertainty relation between pulse duration and bandwidth, it follows that ultrashort laser pulses have a broad spectral width. For example, the spectral width of a 5 fs laser pulse requires the whole visible spectrum. The coherence of femtosecond radiation permits to precisely manipulate the am-

[1] *The notation is adapted to present-day custom and the translation from German to English is taken from ref. [2].*

[a] *Prof. Dr. M. Wollenhaupt, C. Lux, Prof. Dr. T. Baumert*
Universität Kassel
Institut für Physik und CINSaT
Heinrich-Plett-Str. 40
34132 Kassel (Germany)
E-mail: wollenha@physik.uni-kassel.de

[b] *Dr. M. Krug*
OptoMedical Technologies GmbH
Maria-Goeppert-Strasse 1
23562 Lübeck (Germany)

plitude and the phase of the individual spectral components of the pulse by optical Fourier synthesis. By this means, the pulse envelope, the instantaneous frequency and, as of late, even the instantaneous state of polarization of the shaped pulse can be controlled on the femtosecond time scale.[8–10] Under isolated experimental conditions the interaction of coherent laser radiation with matter entails coherent dynamics of matter waves. Manipulation of constructive and destructive interferences of those matter waves forms the basis to exert control on matter by light (as reviewed in monographs[11–14] and special issues[15–19]) and also the key to create designer electron wave packets.[20] In the case of multiphoton ionization the electronic structure of the neutral atoms or molecules can additionally be utilized for the synthesis of shaped free-electron wave packets. The use of intense laser fields extends the options for control through light-induced Stark shifts. To turn the argument on its head, measuring highly structured wave packets being created by suitably shaped laser pulses from the ionization of a molecule will enable one to probe a specific mo-

Prof. Dr. Matthias Wollenhaupt was born in 1965 and studied physics at the University of Göttingen where he did his Diploma on the laser spectroscopy of amorphous solids. He received his Ph.D. at the University of Bielefeld on laser spectroscopic investigations of two-dimensional hypersonic flow fields around re-entry vehicles using planar laser-induced fluorescence (PLIF) on NO molecules. As a post-doc at the Max Planck Institute for Chemistry in Mainz he studied OH radical reactions relevant to atmospheric chemistry by laser photolysis and laser-induced fluorescence (LP/LIF). At the University of Kassel he did his Habilitation on "observation and coherent control of atomic and molecular dynamics". Currently, his research interests range from basic research on strong-field interactions of shaped ultrashort laser pulses with atoms and molecules to applications of femtosecond laser pulses in nonlinear laser microscopy and materials processing.

Dr. Marc Krug was born in 1976 and studied physics at the University of Kassel. In his Diploma he set up a velocity map imaging (VMI) spectrometer for investigations on the interaction of ultrashort polarization-shaped femtosecond laser pulses with alkali metal atoms. At the University of Kassel he received his Ph.D. for measurements of three-dimensional photoelectron angular distributions employing a novel tomographic reconstruction technique. Today he is Chief Operating Officer and Head R&D of OptoMedical Technologies GmbH (Lübeck, Germany), a start-up company that brings imaging and diagnostic methods such as optical coherence tomography to new medical disciplines.

Christian Lux was born in 1984 and studied physics at the University of Kassel. In his diploma, he investigated fragmentation of low-volatility molecules with femtosecond laser pulses in the group of Prof. T. Baumert and Prof. M. Wollenhaupt. He continued this work by employing femtosecond laser techniques for chiral recognition in the gas phase using velocity map imaging and mass spectrometry. Currently Christian Lux is working on his Ph.D. in the same group, studying photoelectron circular dichroism (PECD) through resonance-enhanced multi-photon ionization (REMPI) of chiral molecules.

Prof. Dr. Thomas Baumert was born in 1962 and studied Physics at the University of Freiburg. He obtained his Ph.D., devoted to "Femtosecond Spectroscopy of Molecules and Clusters", with distinction in 1992 and received the Gödecke award. Then he joined the group of Prof. Ahmed Zewail at Caltech for one year and finished his Habilitation in 1997 at the University of Würzburg in the group of Prof. Gustav Gerber with the help of a Habilitation scholarship of Deutsche Forschungsgemeinschaft (DFG) and support by Fonds der Chemischen Industrie (FCI). He was awarded a Heisenberg scholarship by the DFG and joined the German Aerospace Center (Deutsches Zentrum für Luft und Raumfahrt, DLR) in Oberpfaffenhofen where he was head of the light detection and ranging (LIDAR) group until 1999. Then he accepted a full professor position for experimental physics at the University of Kassel. In 2000 he received together with Prof. Gustav Gerber and Dr. Volker Seyfried the Philip Morris Science Award for "Control of Chemical Reactions by Femtosecond Laser Pulses". His research is focused on femtosecond spectroscopy, fundamentals of ultrafast laser control and emerging applications.

lecular structure (for instance different enantiomers) due to highly sensitive interferences.

2. Interference in the Continuum

In the conceptually simplest experiment, the interference of free-electron wave packets has been measured in the photoelectron spectrum by photoionization of potassium atoms (prepared in the 5*p* state by excitation with another laser wavelength) with a coherent femtosecond double pulse.[21] Due to the ionization with the ultrashort laser pulse, a localized outgoing electron wave packet is created in the interaction region at time T_1 as shown in Figure 1a. In vacuum the wave

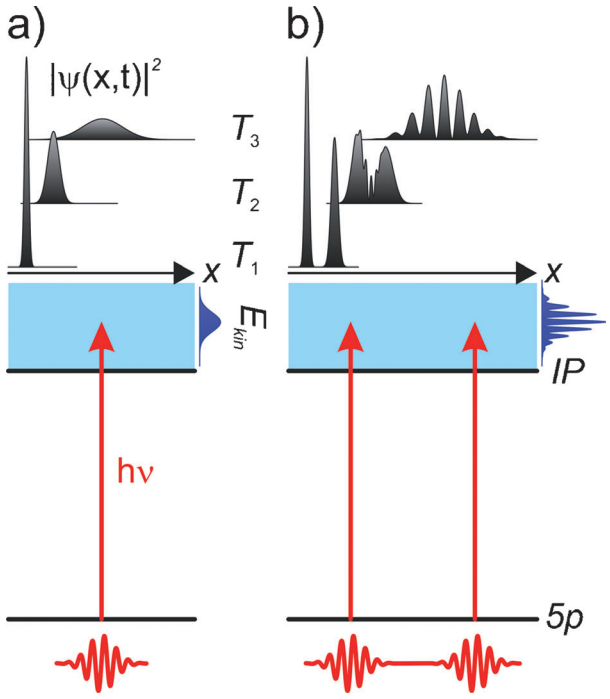

Figure 1. Ionization with femtosecond laser pulses (red) leads to a broad spectrum of photo electron kinetic energies $E_{kin} = h\nu - IP$ (blue photoelectron spectra above the ionization potential *IP*). During its time evolution the single electron wave packet (black in a) broadens in coordinate space as shown for the times $T_1 < T_2 < T_2$. When excited by a coherent double pulse (b) the interference of the two coherent matter waves in the continuum gives rise to the observed interference pattern in the photoelectron spectrum. An analysis of this process in phase space using the Wigner function is presented in Section 3.

packet broadens during its further propagation (T_2 and T_3)—a textbook example of the dispersion of a quantum mechanical matter wave packet (see for example ref. [22]). However, Max Born has pointed out already in 1955 that the dynamics of this wave function can be thought of as a swarm of classical particles with different initial velocities.[23,24] As depicted in Figure 1b, ionization by a coherent double pulse demonstrates most clearly how a structured electron wave packet is created by the interference of the partial wave packets. Since the alkali metal potassium possesses only a single outer electron, one electron at most can be detached during the light–matter interaction. There is a certain probability for ionization during the first laser pulse and the same probability during the second pulse. The double-peaked wave function shown in Figure 1b at T_1 illustrates the corresponding probability amplitude $|\psi(x,t)|^2$. Due to the abovementioned dispersion of matter waves both partial wave packets spread and start to overlap. The interference of both partial wave packets—effectively the interference of the electron with itself—is responsible for the subsequent transient interference pattern at T_2. At some later time (T_3) a quasi-stationary wave packet appears which still broadens, but does not change its qualitative shape. Due to the quadratic dispersion relation of matter waves in vacuum $E(k) = \hbar^2 k^2/2m$ the wave packet evolves into its own spectrum (see Section 3 for an analysis of this relation in Wigner phase space). This is why time-of-flight spectrometers actually measure the momentum distribution $|\tilde{\psi}(k,t)|^2 \propto |\psi(x,t)|^2$ in coordinate space.[25] The time evolution of the wave packet is mathematically described by the fractional Fourier transform, analogously to the diffraction pattern in optics when light waves pass an aperture. In the near field the diffraction pattern changes its shape rapidly (Fresnel diffraction, corresponds to early times in Figure 1) but converges to the stationary Fraunhofer diffraction pattern in the far field. The Fraunhofer diffraction corresponds to late times in Figure 1. Alternatively, the interference of free-electron wave packets can be interpreted as a Young's double-slit [experiment] in the time domain.[21,26] In this picture, the visibility of the interference pattern is complementary to the "which way information" on the photoionization process, that is, the information whether the ionization took place during the first or the second laser pulse. Besides these fundamental aspects of photoionization with coherent laser pulses, interferences in the photoelectron spectrum have become an established tool for attosecond laser pulse characterization.[6,27]

3. Wave-Packet Interference in Phase Space

Now we discuss the time evolution of the double-peaked free-electron wave packet with the help of the Wigner function (Figure 2). The Wigner function $W(x, k, t)$ is a quasi-probability distribution that visualizes the properties of the wave function in phase space.[28] The probability density in coordinate space is obtained by integration along the momentum axis $|\tilde{\psi}(k,t)|^2 = \int W(x, k, t)\, dk$. This quantity shows two separate outgoing partial wave packets directly after the ionization with the coherent double pulse at time T_1. The positive and negative interference terms in the Wigner function (shown in red and blue, respectively) located between the two partial wave packets indicate their mutual coherence. At T_1 those interference terms cancel completely upon integration along the momentum axis and, therefore, the interference of the wave partial packets is not yet visible in coordinate space. For free electrons, that is, in the absence of a potential, the interference pattern in momentum space $|\tilde{\psi}(k,t)|^2 = \int W(x, k, t)dx$, obtained by integration of the Wigner function along the coordinate

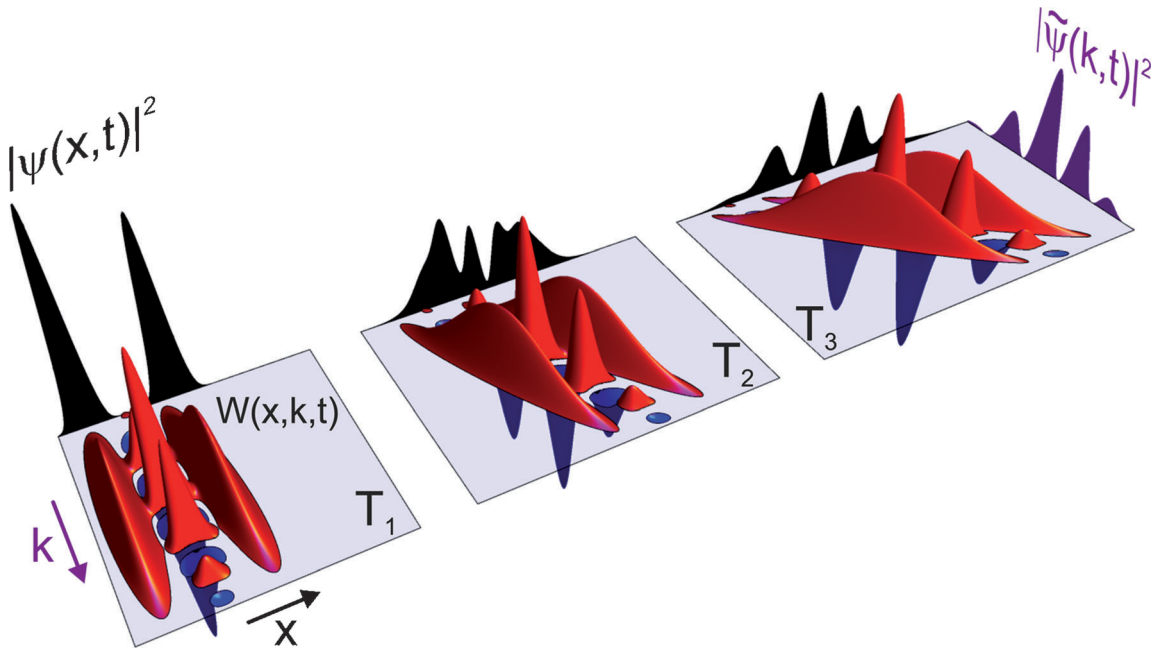

Figure 2. Time evolution of the Wigner function $W(x,k,t)$ (positive values are shown in red, negative values in blue) of a double-peaked free-electron wave packet created by a coherent femtosecond double pulse. The time-dependent probability density in coordinate space $|\psi(x,t)|^2$ (black) is obtained by integration of the Wigner function along the momentum axis whereas momentum distribution $|\tilde{\psi}(k,t)|^2$ (magenta) is obtained by integration along the coordinate axis. The wave packet evolves asymptotically into its own momentum distribution.

axis, is unchanged during the entire time evolution. Since both partial wave packets spread in time due to the dispersion of matter waves in vacuum, the fast components of the second partial wave packet reach the slow components of the first at time T_2. In phase space the initial Wigner function is sheared and therefore the interference terms no longer vanish upon integration along the momentum axis, giving rise to the transient interference pattern in coordinate space. For even larger times (T_3) the Wigner function is sheared to the extent that the interference pattern in coordinate space approaches the stationary interference pattern in momentum space. Due to the quadratic dispersion relation of matter waves in vacuum $E(k) = \hbar^2k^2/2m$ the wave packet evolves asymptotically into its own momentum distribution $|\tilde{\psi}(k,t)|^2 \propto |\psi(x,t)|^2$.

4. Three-Dimensional Control of PADs

In the double-pulse experiment the momentum distribution was structured as a consequence of the interference of two quantum pathways. A much higher degree of control is attainable if the quantum system provides more interfering quantum pathways and complex polarization-shaped laser pulses are used for excitation and ionization. These shaped pulses generate many different partial wave packets which interfere during their coherent time evolution, analogous to the two interfering partial wave packets in the double-pulse experiment. As an example, we consider the resonance-enhanced multiphoton ionization (REMPI) of potassium atoms with polarization-shaped femtosecond laser pulses. Due to the Δl selection rules in this system, the following three quantum pathways for the absorption of the required three light quanta are allowed: $s \rightarrow p \rightarrow d \rightarrow f$, $s \rightarrow p \rightarrow d \rightarrow p$, and $s \rightarrow p \rightarrow s \rightarrow p$ [Figure 3a]. The interference of those pathways, characterized by different dipole moments and different relative phases, creates a superposition

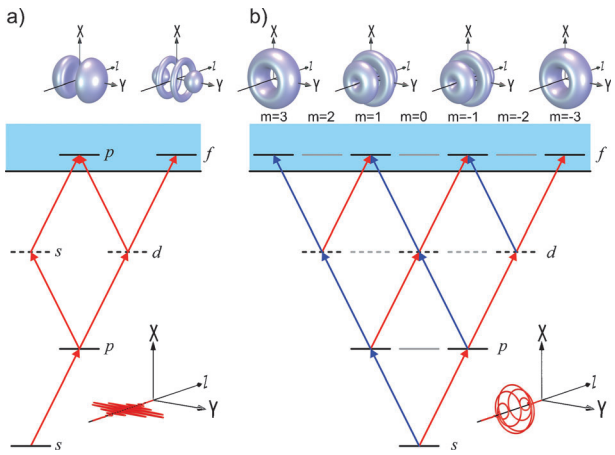

Figure 3. Allowed pathways for multiphoton ionization, which contribute to the interference in the continuum are determined by quantum mechanical selection rules. a) Due to the Δl selection rules resonance enhanced multiphoton ionization (REMPI) of potassium atoms creates superposition states of *p* and *f*-type electron wave packets—shown here for excitation with a linearly polarized laser pulse. b) Superpositions of states with odd value of $m = -3, -1, 1, 3$ are created by ionization with three elliptically polarized photons due to the $\Delta m = \pm 1$ selection rules for elliptically polarized light. The shape of the designer electron wave packets is controlled by the amplitudes and phases of all contributing continuum states. Those amplitudes and phases are determined by the interference of the allowed pathways for multiphoton ionization. The probability of each transition is controlled by the time-dependent ellipticity of the polarization-shaped laser pulse.[33] For simplicity, the fine-structure splitting is not shown.

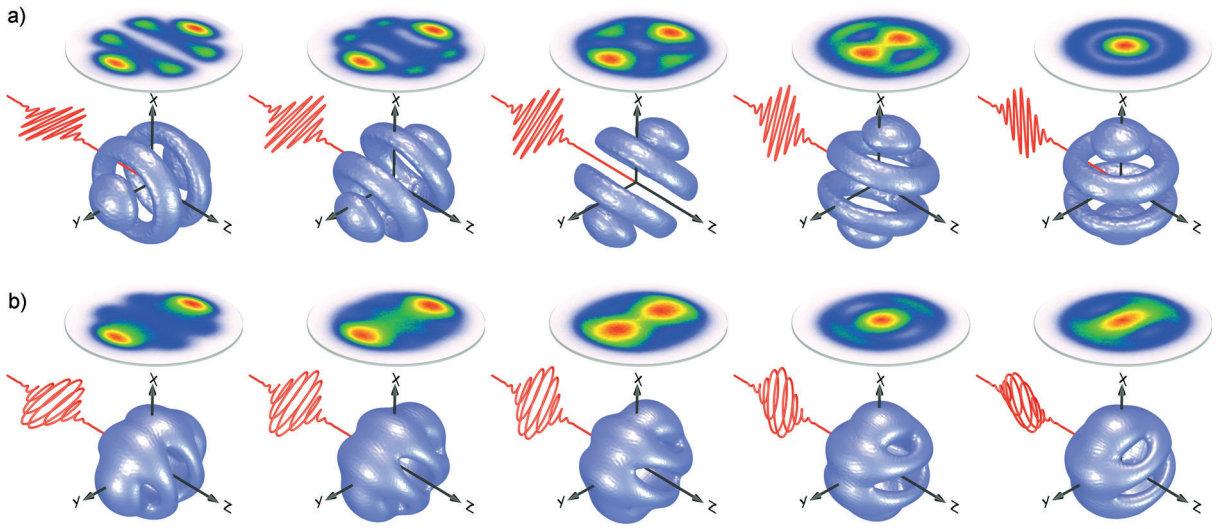

Figure 4. Three-dimensional photoelectron angular distributions (3dPAD) are tomographically reconstructed from measured VMI images. To this end, the polarization vector of the incoming femtosecond laser pulse is rotated about the *z*-axis by 0°, 12°, 22°, 35° and 45° using a $\lambda/2$ plate. a) Three-photon ionization of potassium atoms with a linearly polarized femtosecond laser pulse creates an *f*-type electron wave packet with little *p* contribution. Due to its cylinder symmetry the reconstruction could be compared to the Abel-inverted result, showing excellent agreement.[38] (b) 3dPADs from elliptical polarization violate two prerequisites for the Abel-inversion: firstly, the wave packet is in general rotated out of the *y*–*z*-plane and secondly, it is no longer circular symmetric. However, the tomographic reconstruction reveals a detailed picture of the 3dPAD.

state of *f*-type[2] free-electron wave packets with minor *p* contributions. On the other hand, these interferences of free-electron wave packets from different states could be used to provide a complete description of the photoionization process in terms of transition amplitudes and phases.[29] For example, suitable polarization-shaped pulses could be employed to determine multiphoton ionization matrix elements. Currently, P. Hockett has started to extract these phase shifts from our data.[30] Due to the selection rule $\Delta m = 0$, multiphoton ionization with linearly polarized laser pulses connects any initial $m = 0$ state exclusively with final $m = 0$ states. In contrast, multiphoton ionization using elliptically polarized light with a selection rule $\Delta m = \pm 1$ creates superpositions of different *m* states in the continuum. For example, three-photon ionization of potassium atoms with elliptically polarized light creates superposition states with $m = -3, -1, 1, 3$ (Figure 3b), including all *f*-type electron wave packets, which are just rotated by an angle α about the *z*-axis (Figure 4a)—in agreement with $D^{(3)}_{m'0}(\alpha, \pi/2, 0) = 0$ for all even values of m', where $D^{(l)}_{m',m}(\alpha, \beta, \gamma)$ describes the Wigner matrix[31]—and, in addition, the non-cylindrical symmetric states shown in Figure 4b.[33] In order to excite such a superposition state, eight quantum pathways $s(0) \rightarrow p(-1, 1) \rightarrow d(-2, 0, 2) \rightarrow f(-3, -1, 1, 3)$ are accessible. The absorption of each elliptically polarized photon alters the quantum number by $\Delta m = \pm 1$. The probability for a specific transition is controlled by the corresponding matrix element and the laser polarization. Therefore, in our experiment, three-dimensional control is achieved by the time-dependent polarization of the laser pulse along with the corresponding Δm selection rules and the subsequent interference of the partial electron wave packets in the continuum.

5. Tomographic Reconstruction

In addition to creating designer electron wave packets, measuring their three-dimensional shape, that is, the three-dimensional photoelectron angular distribution (3dPAD), is the next relevant task. Because the 3dPAD contain rich information about the photoionization and intramolecular dynamics, numerous highly differential detection schemes have been developed[29] and recently applied to coherent control.[32–35] An efficient and relatively simple method to measure 3dPADs is to project the complete distribution onto a two-dimensional detector plane. In our experiments, we make use of such a projection technique by employing the velocity map imaging method (VMI).[36] In this scheme photoelectrons created in the interaction region are accelerated in the electric field within a parallel-plate capacitor towards a two-dimensional MCP detector. The detector maps the transversal momentum distribution of the 3dPAD. The motion of the electrons in the spectrometer is described quantum mechanically by the time evolution of the three-dimensional wave packet. In this framework, the measurement of the 3dPAD on the two-dimensional MCP detector is described by the Abel transform.[37] If the wave packet has cylindrical symmetry, a single measurement of a two-dimensional distribution is sufficient to reconstruct the 3dPAD through Abel inversion. For this type of reconstruction it is required that the polarization vector of the light field is

[2] *The term f-type wave packets is used for wave packets with an angular distribution described by the rotated spherical harmonic* $Y_{30}(\theta, \varphi)$. *Because the laser excitation is described in the basis of elliptically polarized light (Figure 3), the f-type wave packets are not aligned along the z-axis, but they actually rotate about the z-axis by an angle of* α *(Figure 4a). Therefore the proper description would be* $R\left(\alpha, \frac{\pi}{2}, 0\right) Y_{30}(\theta, \varphi) = \Sigma_{m'} D^{(3)}_{m',0}\left(\alpha, \frac{\pi}{2}, 0\right) Y_{3m'}(\theta, \varphi)$, *where* $R(\alpha, \beta, \gamma)$ *is a rotation operator parameterized by the Euler angles* α, β, γ *and* $D^{(l)}_{m',m}(\alpha, \beta, \gamma)$ *is the Wigner matrix.*[31]

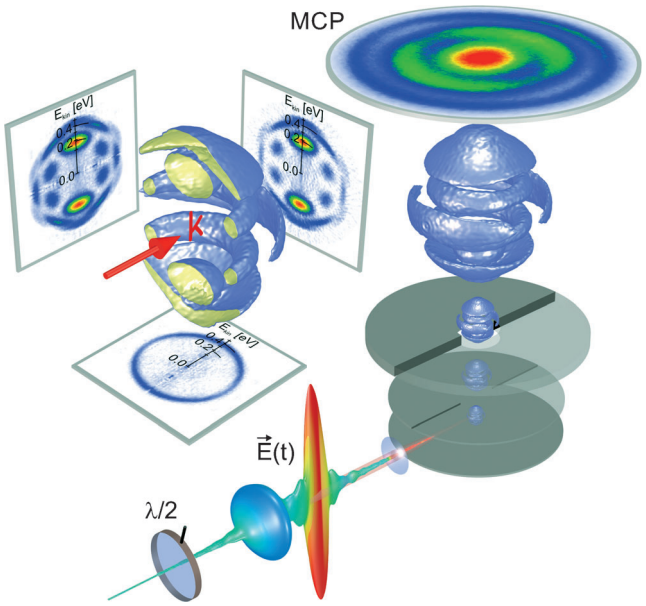

Figure 5. Creation of a designer wave packet through multiphoton ionization with a polarization-shaped femtosecond laser pulse.[20] In order to reconstruct the 3dPAD, its projections are measured on the MCP detector at many different angles. To this end, the incoming polarization-shaped femtosecond laser pulse is rotated about its propagation axis using a $\lambda/2$ plate. The bluish shapes in the VMI represent isosurfaces of the evolving density of the reconstructed free electron wave packet. The polarization-shaped laser pulse is created by our home-built zeptosecond precision pulse shaper.[33,47] The polarization-shaped laser pulse starts with a (with respect to the central frequency) red detuned linearly polarized part and evolves into a blue detuned circularly polarized part. The cut through the distribution shows the interior of the complex three-dimensional distribution. In addition, the energy calibrated electron distributions in the three central planes are projected out.

parallel to the detector plane if linearly polarized light is used. For circularly polarized light the *k*-vector needs to be oriented parallel to the detector plane. Electron wave packets arising from photoionization with elliptically polarized light violate two prerequisites for the Abel inversion: firstly, the wave packet is in general rotated out of the *y*–*z*-plane, and secondly, it is no longer circularly symmetric (Figure 4b).

Recently, a novel approach to measuring 3dPAD of arbitrary shapes by combination of VMI with tomographic techniques was introduced.[38] To this end, the incoming femtosecond laser pulse is rotated using a $\lambda/2$ plate and projections of the 3dPAD are measured at many different angles. In our experiments we typically use 36 projections to cover an angle interval of 180°. Then, a tomography algorithm is used to reconstruct the 3dPAD from the measured projections. Note that for the reconstruction no assumptions on the symmetry of the 3dPAD are required. As visualized in Figure 5, this procedure is also applicable to polarization-shaped laser pulses because the $\lambda/2$ wave plate at an angle of $\theta/2$ rotates any polarization-shaped pulse by an angle of θ since [Eq. (1)]:

$$R\left(\frac{\theta}{2}\right)\cdot J_{\frac{\lambda}{2}}\cdot R^{-1}\left(\frac{\theta}{2}\right)\cdot\begin{pmatrix}\varepsilon_x(t)\\ \varepsilon_y(t)\end{pmatrix}=R(\theta)\cdot\begin{pmatrix}\varepsilon_x(t)\\ -\varepsilon_y(t)\end{pmatrix} \quad (1)$$

where [Eq. (2)]:

$$R(\theta)=\begin{pmatrix}\cos\theta & -\sin\theta\\ \sin\theta & \cos\theta\end{pmatrix} \quad \text{and} \quad J_{\frac{\lambda}{2}}=\begin{pmatrix}1 & 0\\ 0 & -1\end{pmatrix} \quad (2)$$

denote a rotation matrix and a Jones matrix for a $\lambda/2$ waveplate, respectively. The change of the sign of $E_y(t)$ applies to all angles θ and therefore the shape of the pulse $\{E_x(t), -E_y(t)\}^T$ is preserved upon rotation. In order to validate this procedure we generated an *f*-type wave packet by ionization with a linearly polarized laser pulse (Figure 4a) and compared the tomographic reconstruction with the Abel-inverted results. The excellent agreement between the tomographic reconstruction and the Abel inversion reported in ref. [38] confirms the validity of our procedure for cylindrically symmetric wave packets. Recently, this tomographic approach to reconstruct the momentum distribution has been applied to strong-field multiphoton ionization of argon[39] and aligned naphthalene molecules.[40]

6. Intense and Polarization-Shaped Pulses

The reconstruction of a wave packet created by elliptically polarized light (Figure 4b) is a particularly simple example of the interference of the four possible *f*-wave packets $f(-3, -1, 1, 3)$ with different magnetic quantum numbers m (Figure 3b). Much more structured and complex electron wave packets are generated when polarization-shaped pulses are used (Figure 5). Generally speaking, polarization shaping opens the avenue to tailoring the shape of the light pulse to the vectorial properties of the light–matter interaction by adapting the instantaneous state of polarization to the different Δm-allowed transitions and dipole moments which become time dependent during the course of the excitation dynamics.[9] In weak laser fields, the physical mechanism of coherent control of multiphoton excitation is governed by the higher-order spectrum of the modulated pulse. Generally, the higher-order spectrum of a polarization-shaped pulse is not only phase- and polarization-modulated, but also amplitude-modulated. In weak laser fields, the amplitude modulation of the higher-order spectrum explains the modulation of the photoelectron distribution as a function of the excess kinetic energy. However, intense laser pulses, entailing non-perturbative interactions of the light field with the atoms or molecules, provide another effective tool to sculpture the free-electron designer wave packets through skillful manipulation of the bound electron dynamics.

A very efficient strong field control scenario is based on the excitation of a coherent bound electron wave packet—corresponding to a light-induced non-stationary charge oscillation—and a tailored second interaction. In this interaction the light field needs to be tailored to the induced electron dynamics. By applying this control methodology (selective population of dressed states, SPODS) bipolar energy shifts up to hundreds of meV due to the AC–Stark effect have been observed experimentally on atoms.[41,42] Strong-field control by tailored phase

jumps[46] and in particular by SPODS was suggested to be operative in controlling molecules[43–45] as well. The sign of this energy shift is determined by the relative phase between the laser field and the charge oscillation[20] which can be manipulated with zeptosecond precision by our pulse shaper.[47] In this sense, intense fields offer further degrees of freedom to design free-electron wave packets.

7. Adaptive Optimization

Designer electron wave packets are tailored most efficiently if all the above mentioned control scenarios are applied simultaneously. To this end, the laser intensity is used to control strong-field effects, the instantaneous frequency of the pulse controls the kinetic energy of the photoelectrons and the instantaneous state of polarization can be used to manipulate the interferences in the continuum through the excitation and ionization process. Modern pulse-shaping devices with typically 640 pixels for the spectral modulation of each polarization component make available an essentially infinite number of laser pulse shapes. Therefore, in practice, it is very difficult to tailor the laser pulse such that it guides the quantum system most efficiently from the initial to a preselected final state, that is, to find an optimal laser pulse to create a specific designer electron wave packet. One solution to this high-dimensional search space problem is provided by adaptive optimization, for example with the help of genetic algorithms.[48–52] In this iterative procedure the shape of the laser pulse is described by a set of parameters, similar to the genetic code of a biologic individual. The fitness, that is, some measure for the adequacy of the pulse shape with respect to a certain optimization target, is measured in the experiment. Through selection of the best individuals and creation of new pulse shapes that are offspring of those best individuals, optimally adapted pulse shapes are found, analogously to evolution in biology based on "survival of the fittest". Recently, such an adaptive optimization procedure was applied in an experiment to manipulate the two-dimensional projection of a 3dPAD.[20] To this end, a two-dimensional dumbbell-shaped target projection, shown in Figure 6a (labeled T), was defined. Note that almost any arbitrary target function can be chosen, provided it is compatible with energy conservation and the symmetry of the photoionization process. The sequence (1–5) in Figure 6a shows that the measured projections evolve towards the target (T) projection during the optimization procedure. While the measurements of the first generation (1) have some similarity with the projection of an *f*-electron wave packet, see for example Figure 4a, in (2)–(3) the outer maxima of the dumbbell start to emerge. In the course of the optimization procedure the inner part of the dumbbell is filled (4)–(5) such that eventually the measured projection converges to the target function. The result of the three-dimensional tomographic reconstruction of the electron wave packet for the optimal laser pulse is shown in Figure 6b. Inspection of the polarization-shaped pulse (Figure 6c) that produces the optimal wave packet gives clues to the underlying physical mechanisms.

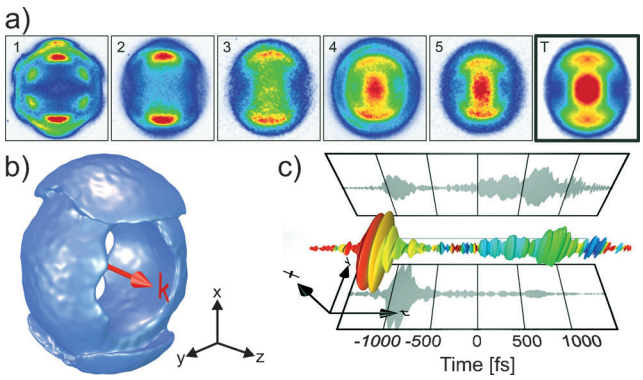

Figure 6. Adaptive optimization of the projection of a 3dPAD. a) Parts 1–5 show the evolution of the optimization of the measured projections towards the target projection (T). b) Tomographic reconstruction of the 3dPAD for the optimized polarization-shaped pulse (c).

8. Applications to Chiral Molecules

The systematic creation of designer electron wave packets with femtosecond laser pulses along with detection through VMI can be used to identify tiny differences in the electronic structure of molecules consisting of identical components. Building on the experiments on circular dichroism in the ion

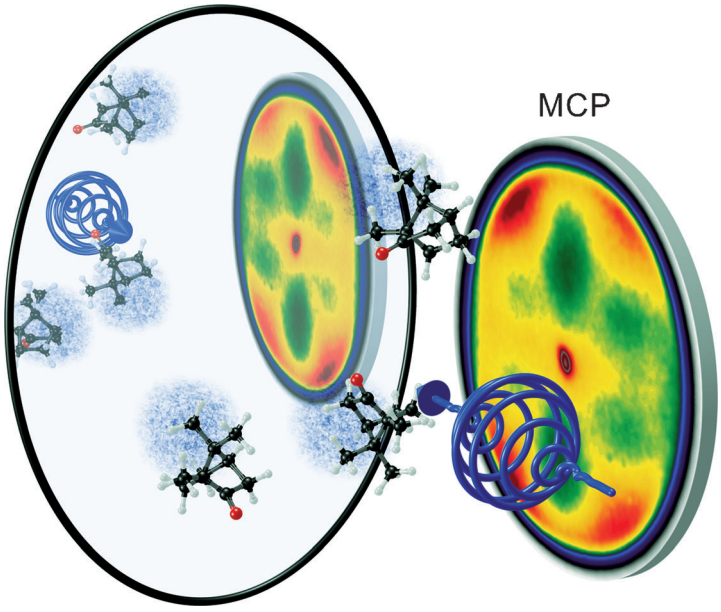

Figure 7. Measurement of the circular dichroism in the multiphoton ionization of randomly oriented camphor molecules.[58] Photoionization with left-handed circularly polarized laser pulses at 400 nm leads to preferential ionization of chiral *R*-(+)-camphor molecules in the propagation direction of the light pulse. The preferential direction of the photoelectrons is detected on the MCP (false color representation of the measured intensity distribution) and visualized by the blue electron clouds. The mirror image of the experiment shows the result of the photoionization of *S*-(−)-camphor being the mirror image of *R*-(+)-camphor.

yield by REMPI[53] and the single-photon synchrotron studies[54–57] employing photoelectron detection, the potential of measuring PAD in the laboratory frame on randomly oriented molecules was recently demonstrated on the circular dichroism from femtosecond REMPI of chiral camphor and fenchone molecules.[58] In those experiments a pronounced asymmetry of up to ± 15 percent was observed in the PADs in forward/backward direction with respect to the propagation direction of the exciting circularly polarized femtosecond laser pulses (Figure 7). Owing to the excellent signal-to-noise ratio of the measured images the asymmetry was already visible in the raw data. In addition, due to the multiphoton nature of the excitation process, higher-order Legendre polynomials have been observed in the angular distribution of the photoelectrons. Similar effects confirming these observations have recently been reported, making use of sophisticated coincidence techniques.[59] Note that circular dichroism was also observed in the ionization yield after multiphoton ionization.[60–62] As this effect is attributed to the interaction of magnetic and electric dipole moments, it is usually smaller than the effect observed in the photoelectron angular distribution, being attributed to a pure electric dipole effect.[63] The results on the multiphoton PECD of chiral molecules such as camphor and fenchone are an important step towards highly sensitive analytical techniques for chiral recognition in the gas phase[64] and also provide a novel approach to determining the absolute configuration of chiral molecules.

9. Conclusions and Outlook

We reviewed the generation and tomographic reconstruction of designer electron wave packets. These designer free-electron wave packets were generated through multiphoton ionization of potassium atoms using polarization-shaped femtosecond laser pulses. The physical mechanism for the design of these three-dimensional free-electron wave packets was elucidated for this prototype system. It turned out that control was achieved by the interplay of Δm selection rules and the time-dependent polarization of the laser pulse, allowing one to manipulate the subsequent interference of the partial electron wave packets in the continuum. Due to the multiphoton nature of the photoionization process, both the electronic structure of the neutral and interference of matter wave packets in the continuum contribute to the final shape. In addition, a novel experimental approach for the measurement of three-dimensional photoelectron angular distributions (3dPAD) based on the combination of the established technique of velocity map imaging (VMI) with a tomographic reconstruction method was described. This novel reconstruction technique can be employed to characterize the 3dPAD in the laboratory frame as well as in the molecular frame of larger molecules. Since only molecules with a favorable orientation with respect to the laser polarization are preferentially excited, selection of those molecules out of the randomly oriented molecular ensemble is the key to measurements in the molecular frame. Therefore, our approach provides a measurement technique complementary to highly differential coincidence techniques and is applicable independently both of whether the ionization is accompanied by dissociation or whether the fragmentation faithfully maps the orientation of the parent molecule. Alternatively, molecular 3dPAD can be measured by application of other alignment techniques—for example laser methods again[40]—prior to photoionization. Due to its sensitivity to electronic structure, this method can be further developed to highly sensitive analytic techniques in the gas phase, for instance for the identification of chiral molecules. Currently, we are investigating the use of coherent control techniques for enhanced chiral recognition. Initially, designer electron wave packets have been a fascinating subject in basic research, but it turns out that they can also play an important role in the development of novel and safe drugs in pharmaceutical industry.

Acknowledgements

Part of this work was published in Physik Journal ***2012***, 11, *37 in German and was translated into English, adapted and extended by the authors. We gratefully acknowledge the financial support by the Deutsche Forschungsgemeinschaft DFG.*

Keywords: chirality · femtosecond pulse shaping · photoelectron spectroscopy · resonance enhanced multiphoton ionization · tomography · velocity map imaging

[1] A. Einstein, *Ann. Phys.* **1905**, *17*, 132 – 148.
[2] D. Ter Haar, *The Old Quantum Theory*, Pergamon, Oxford, **1967**, pp. 91 – 107.
[3] A. Assion, M. Geisler, J. Helbing, V. Seyfried, T. Baumert, *Phys. Rev. A* **1996**, *54*, R4605 – R4608.
[4] A. Stolow, A. E. Bragg, D. M. Neumark, *Chem. Rev.* **2004**, *104*, 1719 – 1757.
[5] M. Wollenhaupt, V. Engel, T. Baumert, *Annu. Rev. Phys. Chem.* **2005**, *56*, 25 – 56.
[6] P. B. Corkum, F. Krausz, *Nat. Phys.* **2007**, *3*, 381 – 387.
[7] C. Davisson, L. H. Germer, *Phys. Rev.* **1927**, *30*, 705 – 740.
[8] M. Wollenhaupt, A. Assion, T. Baumert, *Springer Handbook of Lasers and Optics* (Ed.: F. Träger), Springer, New York, **2007**, pp. 937 – 983.
[9] T. Brixner, G. Krampert, T. Pfeifer, R. Selle, G. Gerber, M. Wollenhaupt, O. Graefe, C. Horn, D. Liese, T. Baumert, *Phys. Rev. Lett.* **2004**, *92*, 208301.
[10] A. M. Weiner, *Opt. Commun.* **2011**, *284*, 3669 – 3692.
[11] S. A. Rice, M. Zhao, *Optical Control of Molecular Dynamics*, Wiley, New York, **2000**.
[12] M. Shapiro, P. Brumer, *Quantum Control of Molecular Processes*, Wiley-VCH, Weinheim, **2012**.
[13] D. Tannor, *Introduction to Quantum Mechanics: A Time-Dependent Perspective*, Palgrave Macmillan Limited, Sausalito, **2007**.
[14] T. Brixner, T. Pfeifer, G. Gerber, M. Wollenhaupt, T. Baumert, *Femtosecond Laser Spectroscopy* (Ed.: P. Hannaford), Springer, New York, **2005**, pp. 225 – 266.
[15] T. Baumert, J. Helbing, G. Gerber, *Adv. Chem. Phys.* **1997**, *101*, 47 – 82.
[16] J. L. Herek, *J. Photochem. Photobiol. A* **2006**, *180*, 225.
[17] H. Fielding, M. Shapiro, T. Baumert, *J. Phys. B: At. Mol. Opt. Phys.* **2008**, *41*, 070201.
[18] H. Rabitz, *New J. Phys.* **2009**, *11*, 105030.
[19] H. H. Fielding, M. A. Robb, *Phys. Chem. Chem. Phys.* **2010**, *12*, 15569.
[20] M. Wollenhaupt, T. Baumert, *Faraday Discuss.* **2011**, *153*, 9 – 26.
[21] M. Wollenhaupt, A. Assion, D. Liese, C. Sarpe-Tudoran, T. Baumert, S. Zamith, M. A. Bouchene, B. Girard, A. Flettner, U. Weichmann, G. Gerber, *Phys. Rev. Lett.* **2002**, *89*, 173001.
[22] C. Cohen-Tannoudji, B. Diu, F. Laloë, *Quantum Mechanics, Vol. 1*, Wiley, Paris, **1977**.

[23] M. Born, *Phys. Bl.* **1955**, *2*, 49 – 54.
[24] M. Nauenberg, *The Physics and Chemistry of Wave Packets* (Eds.: J. A. Yeazell, T. Uzer), Wiley, New York, **2000**, pp. 1 – 29.
[25] M. Winter, M. Wollenhaupt, T. Baumert, *Opt. Commun.* **2006**, *264*, 285 – 292.
[26] F. Lindner, M. G. Schätzel, H. Walther, A. Baltuška, E. Goulielmakis, F. Krausz, D. B. Milošević, D. Bauer, W. Becker, G. G. Paulus, *Phys. Rev. Lett.* **2005**, *95*, 040401.
[27] J. Mauritsson, T. Remetter, M. Swoboda, K. Klünder, A. L'Huillier, K. J. Schafer, O. Ghafur, F. Kelkensberg, W. Siu, P. Johnsson, M. J. J. Vrakking, I. Znakovskaya, T. Uphues, S. Zherebtsov, M. F. Kling, F. Lépine, E. Benedetti, F. Ferrari, G. Sansone, M. Nisolo, *Phys. Rev. Lett.* **2010**, *105*, 053001.
[28] W. P. Schleich, *Quantum Optics in Phase Space*, Wiley-VCH, Weinheim, **2001**.
[29] K. L. Reid, *Mol. Phys.* **2012**, *110*, 131 – 147.
[30] P. Hockett, *private communication*.
[31] A. R. Edmonds, *Angular Momentum in Quantum Mechanics, 2nd ed., 4th printing*, Princeton University Press, Princeton, **1996**.
[32] M. Krug, T. Bayer, M. Wollenhaupt, C. Sarpe-Tudoran, T. Baumert, S. S. Ivanov, N. V. Vitanov, *New J. Phys.* **2009**, *11*, 105051.
[33] M. Wollenhaupt, M. Krug, J. Köhler, T. Bayer, C. Sarpe-Tudoran, T. Baumert, *Appl. Phys. B. Lasers Opt.* **2009**, *95*, 245 – 259.
[34] D. A. Malik, A. T. J. B. Eppink, W. L. Meerts, A. V. Kimel, A. Kirilyuk, T. Rasing, W. J. van der Zande, *Phys. Rev. A* **2011**, *84*, 043404.
[35] A. Vredenborg, C. S. Lehmann, D. Irimia, W. G. Roeterdink, M. H. M. Janssen, *ChemPhysChem* **2011**, *12*, 1459 – 1473.
[36] A. T. J. B. Eppink, D. H. Parker, *Rev. Sci. Instrum.* **1997**, *68*, 3477 – 3484.
[37] G. A. Garcia, L. Nahon, I. Powis, *Rev. Sci. Instrum.* **2004**, *75*, 4989 – 4996.
[38] M. Wollenhaupt, M. Krug, J. Köhler, T. Bayer, C. Sarpe-Tudoran, T. Baumert, *Appl. Phys. B. Lasers Opt.* **2009**, *95*, 647 – 651.
[39] C. Smeenk, L. Arissian, A. Staude, D. M. Villeneuve, P. B. Corkum, *J. Phys. B* **2009**, *42*, 185402.
[40] J. Maurer, D. Dimitrovski, L. Christensen, L. B. Madsen, H. Stapelfeldt, *Phys. Rev. Lett.* **2012**, *109*, 123001.
[41] M. Wollenhaupt, D. Liese, A. Präkelt, C. Sarpe-Tudoran, T. Baumert, *Chem. Phys. Lett.* **2006**, *419*, 184 – 190.
[42] T. Bayer, M. Wollenhaupt, T. Baumert, *J. Phys. B* **2008**, *41*, 074007.
[43] M. Wollenhaupt, T. Baumert, *J. Photochem. Photobiol. A* **2006**, *180*, 248 – 255.
[44] P. von den Hoff, M. Kowalewski, R. de Vivie-Riedle, *Faraday Discuss.* **2011**, *153*, 159 – 171.
[45] J. Petersen, R. Mitrić, *Phys. Chem. Chem. Phys.* **2012**, *14*, 8299 – 8306.
[46] R. Kosloff, A. D. Hammerich, D. Tannor, *Phys. Rev. Lett.* **1992**, *69*, 2172 – 2175.
[47] J. Köhler, M. Wollenhaupt, T. Bayer, C. Sarpe, T. Baumert, *Opt. Express* **2011**, *19*, 11638 – 11653.
[48] R. S. Judson, H. Rabitz, *Phys. Rev. Lett.* **1992**, *68*, 1500 – 1503.
[49] T. Baumert, T. Brixner, V. Seyfried, M. Strehle, G. Gerber, *Appl. Phys. B. Lasers Opt.* **1997**, *65*, 779 – 782.
[50] C. J. Bardeen, V. V. Yakovlev, K. R. Wilson, S. D. Carpenter, P. M. Weber, W. S. Warren, *Chem. Phys. Lett.* **1997**, *280*, 151 – 158.
[51] D. Yelin, D. Meshulach, Y. Silberberg, *Opt. Lett.* **1997**, *22*, 1793 – 1795.
[52] A. Assion, T. Baumert, M. Bergt, T. Brixner, B. Kiefer, V. Seyfried, M. Strehle, G. Gerber, *Science* **1998**, *282*, 919 – 922.
[53] C. Logé, A. Bornschlegl, U. Boesl, *Anal. Bioanal. Chem.* **2009**, *395*, 1631 – 1639.
[54] N. Böwering, T. Lischke, B. Schmidtke, N. Müller, T. Khalil, U. Heinzmann, *Phys. Rev. Lett.* **2001**, *86*, 1187 – 1190.
[55] G. A. Garcia, L. Nahon, M. Lebech, J.-C. Houver, D. Dowek, I. Powis, *J. Chem. Phys.* **2003**, *119*, 8781 – 8784.
[56] S. Turchini, N. Zema, G. Contini, G. Alberti, M. Alagia, S. Stranges, G. Fronzoni, M. Stener, P. Decleva, T. Prosperi, *Phys. Rev. A* **2004**, *70*, 014502.
[57] I. Powis, *Adv. Chem. Phys.* **2008**, *138*, 267 – 329.
[58] C. Lux, M. Wollenhaupt, T. Bolze, Q. Liang, J. Köhler, C. Sarpe, T. Baumert, *Angew. Chem.* **2012**, *124*, 5086 – 5090; *Angew. Chem. Int. Ed.* **2012**, *51*, 5001 – 5005.
[59] N. Bhargava Ram, C. S. Lehmann, M. H. M. Janssen, *Eur. Phys. J.* **2012**, in print.
[60] U. Boesl von Grafenstein, A. Bornschlegl, *ChemPhysChem* **2006**, *7*, 2085 – 2087.
[61] R. Li, R. Sullivan, W. Al-Basheer, R. M. Pagni, R. N. Compton, *J. Chem. Phys.* **2006**, *125*, 144304.
[62] H. G. Breunig, G. Urbasch, P. Horsch, J. Cordes, U. Koert, K.-M. Weitzel, *ChemPhysChem* **2009**, *10*, 1199 – 1202.
[63] B. Ritchie, *Phys. Rev. A* **1976**, *14*, 359 – 362.
[64] A. Zehnacker in *Chiral Recognition in the Gas Phase* (Ed.: A. Zehnacker), CRC, Boca Raton, **2010**.

Received: November 22, 2012
Published online on March 25, 2013